

To be submitted to
Nuclear Physics

ISTITUTO NAZIONALE DI FISICA NUCLEARE
Laboratori Nazionali di Frascati

LNF-79/32(P)
29 Maggio 1979

F. Balestra, M.P. Bussa, L. Busso, I.V. Falomkin,
R. Garfagnini, C. Guaraldo, A. Maggiora, G. Piragino,
G.B. Pontecorvo, R. Scrimaglio and Yu.A. Shcherbakov:
 π^+ MESONS INTERACTION ON ${}^4\text{He}$ AT 120, 145 AND 165 MeV.

F. Balestra^(x), M. P. Bussa^(x), L. Busso^(x), I. V. Falomkin^(o),
R. Garfagnini^(x), C. Guaraldo, A. Maggiora, G. Piragino^(x),
G. B. Pontecorvo^(o), R. Scrimaglio and Yu. A. Shcherbakov^(o):
 π^+ MESONS INTERACTION ON ^4He AT 120, 145 AND 165 MeV.

ABSTRACT.

The total cross sections and the differential cross sections of the (π^+ , ^4He) elastic and inelastic reactions at $E_\pi = 120, 145$ and 165 MeV have been measured using a 38 cm diffusion cloud chamber in magnetic field exposed to the Frascati Laboratories pion beam. Total π^+ track lengths of $(2141 \pm 10) \times 10^3$ cm, $(3435 \pm 10) \times 10^3$ cm and $(2413 \pm 10) \times 10^3$ cm were measured at the three considered energies, respectively. The elastic cross section data are in good agreement with the results of the Dubna-Torino collaboration. The total inelastic cross sections have been obtained taking into account the contributions from all the inelastic channels. The analysis of the various inelastic processes has allowed to distinguish five main reaction mechanisms, which compare reasonably with the existing data and with the models on pion-light nuclei interaction.

(x) Istituto di Fisica dell'Università di Torino, and INFN, Sezione di Torino.

(o) Joint Institute for Nuclear Research, Dubna (USSR).

1. - INTRODUCTION.

The (π^+ , ^4He) elastic and inelastic reactions at $E_\pi = 120, 145$ and 165 MeV have been investigated by means of a diffusion cloud chamber in magnetic field. In this paper the final results of the analysis of differential and total cross sections measurements are reported.

The total elastic cross sections have been obtained from the angular distributions in the 20° - 180° interval by integrating the best fit with Legendre polynomials extrapolated to zero degrees. The total inelastic cross sections and the total cross section values have been obtained taking into account the contributions from all the inelastic channels. The analysis of the inelastic reactions allowed to ascribe them to five main processes: 1) Multiple scattering processes, in which the final state particles are the result of successive collisions of the meson with the nucleons in a cascade process. 2) Quasi deuteron absorption of the π^+ followed by two fast protons emission. 3) Isobaric resonance excitation in the nucleus in single-nucleon removal reactions (knock out and charge exchange). 4) Three-nucleon exchange mechanism in addition to the one-nucleon mechanism in knock out and charge exchange reactions. 5) Clustering effects stressed by strong correlations between particles and recoil nucleus in the final state.

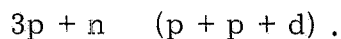
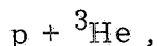
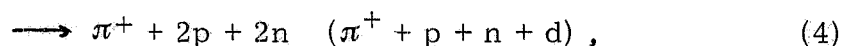
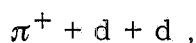
All these processes have been separately investigated in connection with the obtained experimental results.

In Section 2 the experimental procedure is reported. In Section 3 the total elastic cross sections are discussed. Section 4 concerns inelastic processes: multiple scattering processes (4. 1); quasi deuteron absorption in non radiative capture (4. 2); isobaric resonance excitation (4. 3); three-nucleon exchange mechanism (4. 4); clustering effects (4. 5).

2. - EXPERIMENTAL PROCEDURE.

We have studied the interaction of π^+ on ${}^4\text{He}$ with a 38 cm diameter diffusion cloud chamber filled at 15 atm in a magnetic field of 5 KGauss, exposed to the pion beam of Frascati National Laboratories. About 100,000 photographs have been taken. The details of the experimental device are described in ref. (1). The spectra of the π^+ entering into the chamber in different exposures allowed us to study three interaction energies: $E_\pi = (120 \pm 15) \text{ MeV}$, $(145 \pm 10) \text{ MeV}$ and $(165 \pm 10) \text{ MeV}$. The fiducial volume considered was 20 cm (width) x 23 cm (depth) x 5 cm (height) and the vertexes of all the measured events were contained in the 3 cm high central part of this volume. Total π^+ track lengths of $(2141 \pm 10) \times 10^3 \text{ cm}$, $(3435 \pm 10) \times 10^3 \text{ cm}$ and $(2413 \pm 10) \times 10^3 \text{ cm}$ were measured at the incident pion energies $E_\pi = 120, 145$ and 165 MeV , respectively.

The following reactions have been taken into account:



For all the events, the angles between the outgoing charged particles and the incident pion have been measured with an error lower than 1 degree, the ranges (when possible) with an error lower than 1 mm and the radius of curvature of the tracks with an error depending on track length and radius values^(1, 2). The comparison between the ionization of the outgoing particle tracks and that of the incident

pion, together with the curvature measurements, allowed to separate slow pion from fast proton tracks and proton tracks from ^3H and ^3He tracks.

The $(\pi^+ n \ ^3\text{He})$ reaction has been separated from the elastic scattering channel by the criteria described in ref. (3) (preliminary results).

As known, it is not possible to distinguish proton tracks from deuteron tracks⁽⁴⁾ and to separate the reactions with emission of a deuteron from those with emission of a (n-p) pair. As a consequence, the $(\pi^+ pnd)$ reaction was not distinguished from the $(\pi^+ 2p 2n)$ reaction and the (ppd) reaction was not separated from the $(3pn)$ reaction. However, taking into account the small binding energy of the deuteron, it is possible to assume that the probability of a reaction with emission of one or more deuterons is very small. This assumption is also supported by the experimental results of ref. (5) and (6). As far as the $(\pi^+ dd)$ reaction is concerned no statistical evidence was found.

Also, no statistical evidence was found for the double charge exchange $(\pi^- 4p)$ reaction.

For the two last groups of reactions (6) and (7), it was not possible to separate with certainty the single charge exchange event from the single absorption event. But with a complete kinematical analysis of each event and with the aid of the FOWL Program⁽⁷⁾, it was possible to calculate phase space distributions of particles through the Monte Carlo method and to evaluate the relative distributions of the two classes of events.

In Table I the total cross section for all the considered reactions are reported.

3. - TOTAL ELASTIC CROSS SECTION.

The total elastic cross section values at 120, 145 and 165 MeV, are reported in Table I. These values have been obtained from differential cross section measurements in the 20° - 180° interval, by integrating the best fit with Legendre polynomials extrapolated to zero degrees.

TABLE I

Total elastic and inelastic cross sections (mb) in the $(\pi^+ {}^4\text{He})$ interaction.

E_π (MeV)	$(\pi^+ {}^4\text{He})$	$(\pi^+ n {}^3\text{He})$	$(\pi^+ p {}^3\text{H})$	$(\pi^+ 2p 2n)$	$(\pi^0 p {}^3\text{He})$	(3pn)	σ_{inel}	σ_{tot}
120 ± 15	77 ± 10	31 ± 5	74 ± 10	38 ± 9	23 ± 7	11 ± 4	177 ± 18	254 ± 19
145 ± 10	90 ± 9	46 ± 5	73 ± 8	28 ± 6	28 ± 6	12 ± 4	187 ± 13	277 ± 15
165 ± 10	112 ± 11	75 ± 8	107 ± 12	26 ± 7	47 ± 10	11 ± 4	266 ± 20	378 ± 21

The cross sections are in rather good agreement with the results of the Dubna-Torino collaboration⁽⁸⁾, in the energy interval 68-156 MeV.

In Fig. 1 the present data are compared with those of ref. (8), with the data of Fowler et al.⁽⁹⁾ at 60 MeV, the data of Kozodaev et al.⁽⁵⁾ at 273 MeV and with the low energy data of Crowe et al.⁽¹⁰⁾ (at 50, 60, 70, 75 MeV) and Nordberg et al.⁽¹¹⁾ (at 24 MeV) we deduced

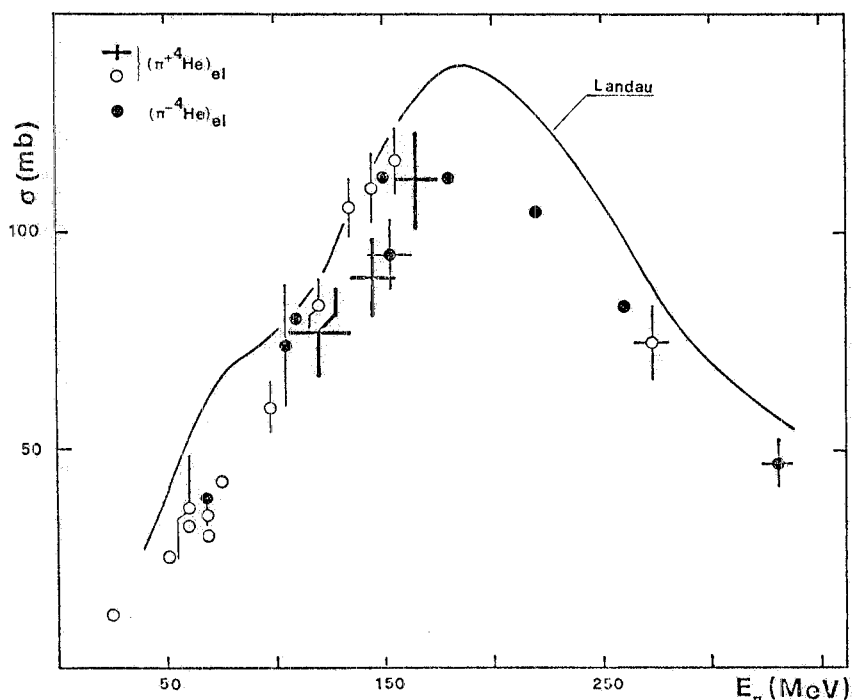


FIG. 1 - $(\pi^+, {}^4\text{He})$ total elastic cross section versus pion energy. Crosses: present data. Open circles: from refs. (5, 8, 9, 10, 11). Full circles: $(\pi^-, {}^4\text{He})$ total elastic cross section data from refs. (4, 5, 9, 12). The full line is the result of the total elastic cross section Landau calculation⁽¹³⁾.

from the differential cross sections by integrating the best fits with Legendre polynomials. For comparison, the $(\pi^-, {}^4\text{He})$ data of Binon et al.⁽¹²⁾ in the energy interval 70-260 MeV, the Fowler et al.⁽⁹⁾ data at 105 MeV, the Budagov et al.⁽⁴⁾ data at 153 MeV and the Kozodaev et al.⁽⁵⁾ data at 330 MeV are also reported in the figure.

Several optical model calculations of the pion- ${}^4\text{He}$ scattering have been performed. In Fig. 1 the full line represents the total elastic cross section energy behaviour obtained by Landau⁽¹³⁾. The experimental behaviour is qualitatively reproduced, however the theoretical values are systematically higher than the experimental ones for $E_\pi \lesssim 100$ MeV and $E_\pi \gtrsim 160$ MeV. Similar results have been obtained by Wakamatsu⁽¹⁴⁾ and by Maillet et al.⁽¹⁵⁾.

4. - TOTAL INELASTIC CROSS SECTIONS.

The total and total inelastic cross sections at 120, 145 and 165 MeV, are reported in Table I. In the Table the total cross section values are also reported.

In Fig. 2 the present total inelastic data are compared with the only total inelastic existing data of Fowler et al.⁽⁹⁾ (at 60 MeV) and Kozodaev et al.⁽⁵⁾ (at 273 MeV). Moreover, the present total cross section data are compared with the total cross section values of Fowler et al.⁽⁹⁾, of Kozodaev et al.⁽⁵⁾, of Binon et al.⁽¹²⁾ (at 110 MeV) and of Wilkin et al.⁽¹⁶⁾ in the energy interval 110-265 MeV. The agreement between the new total cross section data and those obtained by Wilkin et al.⁽¹⁶⁾ in the same energy interval seems to be rather good within the different errors.

The total cross section calculation by Landau⁽¹³⁾ reproduces the experimental behaviour with only a light difference in the peak position. Similar results have been obtained in refs. (14, 15).

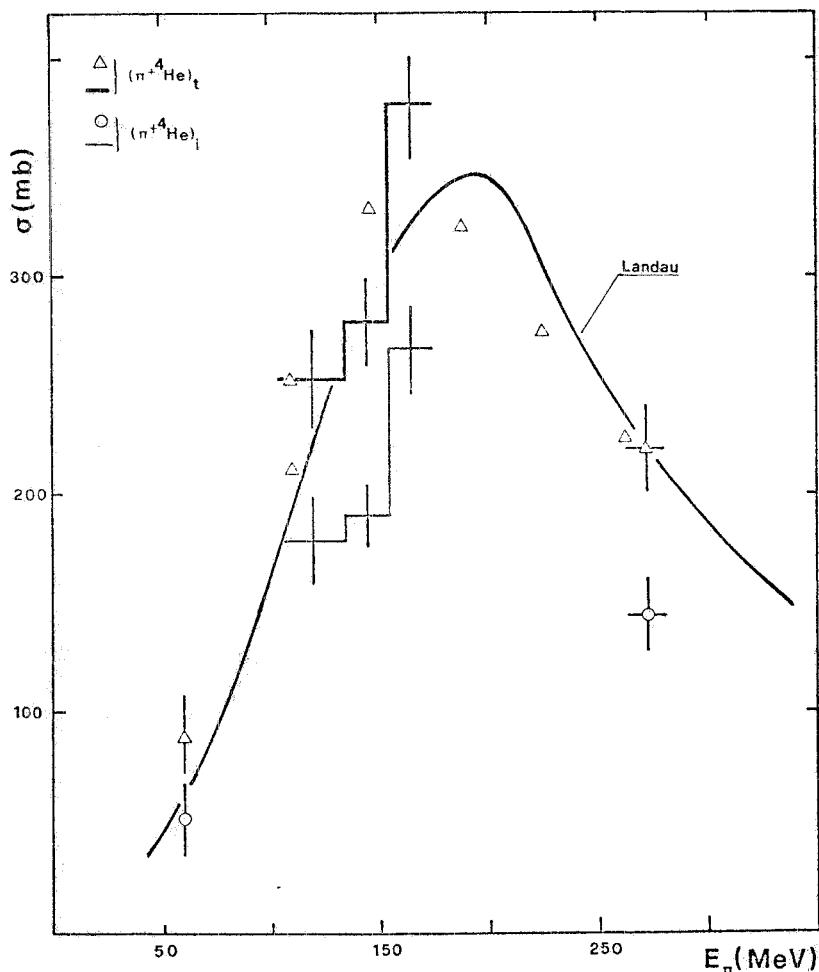
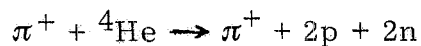


FIG. 2 - $(\pi^+, {}^4\text{He})$ total and total inelastic cross sections versus pion energy. Crosses: present data. Open circles: total inelastic data from refs. (5, 9). Triangles: total cross section data from refs. (5, 9, 12, 16). The full line is the result of the total cross section Landau calculation⁽¹³⁾.

4. 1. - Multiple scattering processes.

The cross section values of the reaction



at 120, 145 and 165 MeV are reported in Table I.

The mechanism of this reaction can be interpreted in two ways. Firstly, the reaction can be the result of simultaneous interactions between pion and complexes of nucleons. This assumption is supported by the fact that the main mechanism in non radiative capture of π^+ on

${}^4\text{He}$ does result in quasi-deuteron absorption, i. e. in processes in which at least two nucleons participate. Secondly, this case can be the result of successive collisions of the meson with the nucleons, justifying the terminology adopted tentatively by Kozodaev et al.⁽⁵⁾ of "multiple scattering processes". In this last case, since no correlation is effective, the angular distribution of the particles in the final state is expected to be isotropic. Actually, it is probable that both processes are in operation.

Fig. 3, upper part, compares the present ($\pi^+ 2p 2n$) data with the existing one obtained by Kozodaev et al.⁽⁵⁾ at 273 MeV and with the ($\pi^- 2p 2n$) data of Budagov et al.⁽⁴⁾ at 153 MeV and of Kozodaev et al.⁽⁵⁾ at 330 MeV.

Fig. 3, central part, shows the distribution of ($\pi^+ 2p 2n$) events as a function of the opening angle between the two protons, at $E_\pi = 145$ MeV. The behaviour is nearly isotropic, indicating that in this reaction the cascade process does take place and seems to be the predominant one.

This conclusion is also stressed in Fig. 3, lower part, in which the differential cross section at $E_\pi = 145$ MeV versus the angle of the scattered pion is reported. The angular distribution is in agreement, as shown in the figure, with the result obtained using the FOWL Program⁽⁷⁾ to calculate the phase space distribution, with the hypothesis of isotropically scattered particles and without interaction in the final state. On the contrary, in an absorption process, as ${}^4\text{He}(\gamma, 2p 2n)$, a correlation is active between the protons, since they are emitted with large relative angle⁽¹⁷⁾.

It is also possible to give an evaluation of the relative probability ϵ of multiple scattering in inelastic interaction on ${}^4\text{He}$. Reactions such as ($\pi^+ p {}^3\text{H}$) and ($\pi^+ n {}^3\text{He}$) can be interpreted as typical results of a quasi free scattering by individual bound nucleons, considering that the residual nuclei do not participate directly in the interaction with

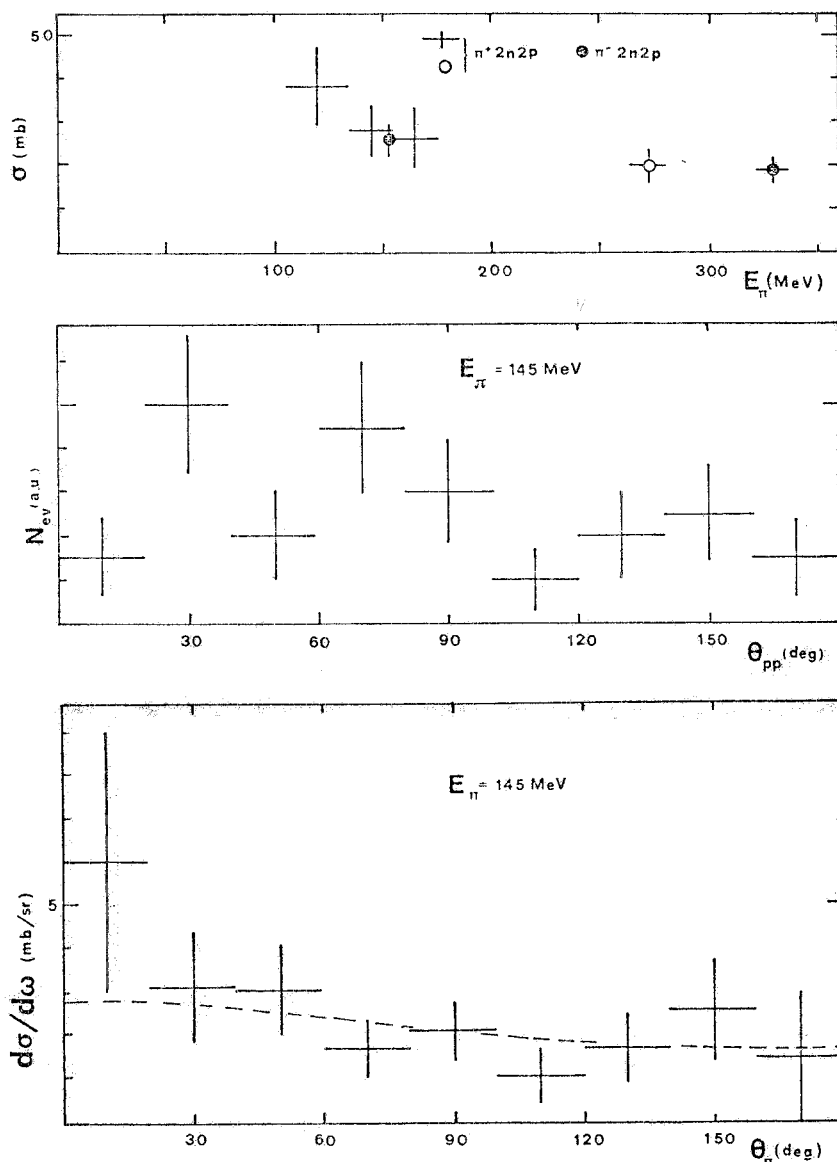


FIG. 3 - Upper part: ${}^4\text{He}(\pi^+, \pi^+ 2p 2n)$ cross section versus pion energy. Crosses: present data. Open circle: from ref. (5). Full circles: ${}^4\text{He}(\pi^-, \pi^- 2p 2n)$ cross section data from refs. (4, 5). Central part; Distribution of $(\pi^+ 2p 2n)$ events versus the opening angle between the two protons at $E_\pi = 145$ MeV. Lower part: ${}^4\text{He}(\pi^+, \pi^+ 2p 2n)$ differential cross section versus the scattered pion angle (crosses) compared with the phase space distribution obtained with the hypothesis of isotropically scattered particles and without interaction in the final state.

the incoming pion. The probability ϵ of multiple scattering can be determined directly from the number of cases that correspond to the above reported reactions:

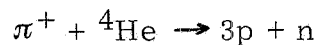
$$\varepsilon = \frac{\sigma(\pi^+ 2p 2n)}{\sigma(\pi^+ 2p 2n) + \sigma(\pi^+ p {}^3\text{H}) + \sigma(\pi^+ n {}^3\text{He})}$$

From Table I, the mean value of ε in the energy region considered, resulted $\varepsilon = (0.20 \pm 0.05)$, to be compared with $\varepsilon = (0.24 \pm 0.06)$ obtained in ref. (5) with 273 MeV π^+ ; $\varepsilon = (0.29 \pm 0.06)$ obtained in ref. (4) with 153 MeV π^- ; $\varepsilon = (0.29 \pm 0.05)$ obtained in ref. (5) with 330 MeV π^- .

It is possible to conclude remarking the relevant role of multiple scattering processes in pion- ${}^4\text{He}$ inelastic interaction, together with their relative independence on energy and pion charge.

4. 2. - Quasi deuteron absorption in non radiative capture.

The cross section values of the reaction



at 120, 145 and 165 MeV are reported in Table I.

The events of this non radiative capture reaction appear as stars of three fast particles. The relative high energy of all the particles indicates that the number of reactions with charge exchange ($\pi^0 3pn$) is negligible respect to the number of (3pn) events.

We selected the two faster particles of each event and they resulted mostly emitted with large relative opening angle, in agreement with the hypothesis of two fast protons emission from π^+ absorption by a quasi deuteron:

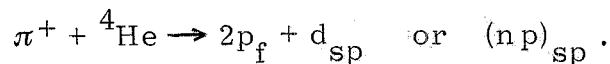


Fig. 4, upper part, shows the distribution of (3pn) events as a function of the opening angle between the two faster protons, at $E_\pi = 145$ MeV. A strong correlation between the two protons is clearly active at large angle. In the figure, the distribution of fast protons

pairs, produced in π^+ absorption in nuclear emulsion at $E_\pi = 45 \text{ MeV}$ ⁽¹⁸⁾, as a function of their opening angle, is also reported. Notwithstanding the different pion energies, the agreement between the distributions is very good and confirms the role of this absorption mechanism. The third charged particle should be as a spectator.

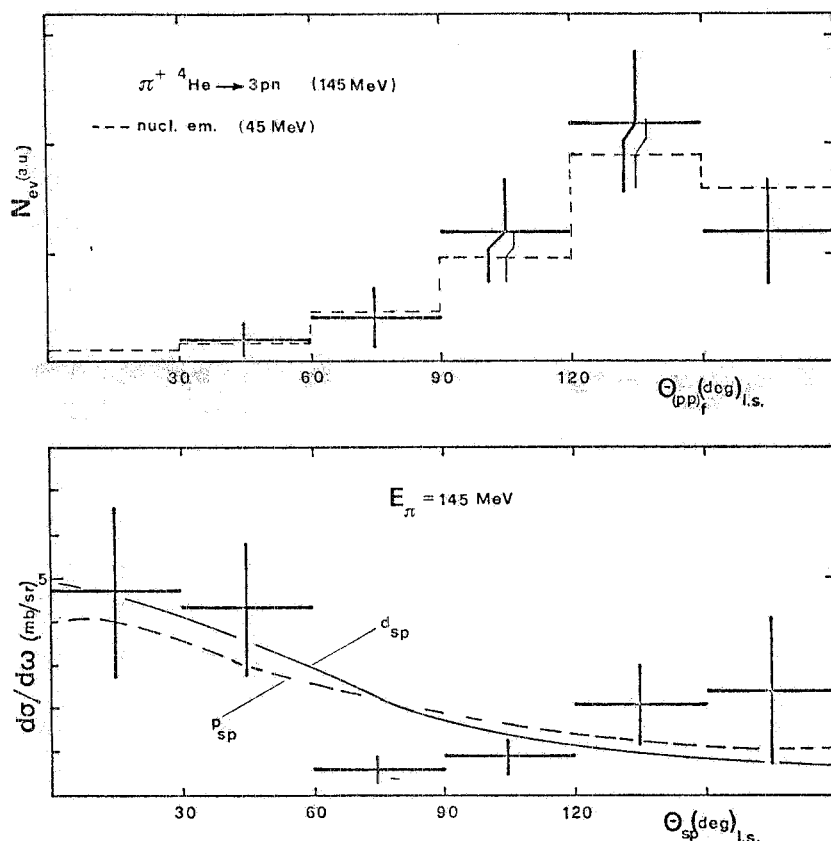


FIG. 4 - Upper part: Crosses: distribution of (3pn) events versus the opening angle between the two faster protons at $E_\pi = 145 \text{ MeV}$. Dashed line: distribution of fast protons pairs produced in π^+ absorption in nuclear emulsion at $E_\pi = 45 \text{ MeV}$. Lower part: ${}^4\text{He}(\pi^+, 3pn)$ differential cross section versus the spectator particle angle (crosses), compared with the phase space distributions obtained with the hypothesis that two protons are emitted with an angle larger than 90° and the spectator particle is a deuteron (full-line) or a proton (dashed-line).

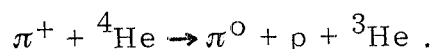
Fig. 4, lower part, shows the angular distribution of the spectator particle, compared with the phase space distribution calculated by the FOWL Program⁽⁷⁾, with the hypothesis that the spectator is a

deuteron or a proton from a (n-p) pair. It is not possible to recognize which is the spectator particle.

Non radiative capture of pions on ${}^4\text{He}$ can also proceed through the channel



which ought to be distinguished from the single charge exchange reaction



In order to separate the two above reactions we tested the coplanarity of p and ${}^3\text{He}$ tracks and deduced all the kinematic parameters in the phase space for the two and the three body reactions.

Fig. 5 shows the experimental distribution at $E_\pi = (145 \pm 10)$ MeV of all the events with a proton and a ${}^3\text{He}$ nucleus in the final state as a

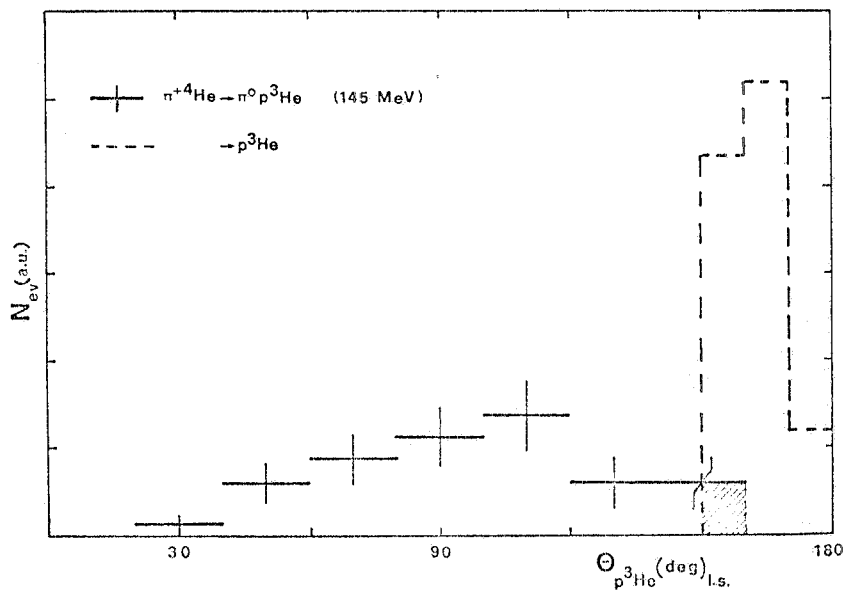


FIG. 5 - Experimental distribution of the events with a proton and a ${}^3\text{He}$ nucleus in the final state, versus the p- ${}^3\text{He}$ opening angle at $E_\pi = (145 \pm 10)$ MeV (crosses), compared with the phase space distribution calculated for $(p^3\text{He})$ events (dashed line). The dashed area represents the fraction of the measured events which belongs to the absorption reaction without charge exchange ${}^4\text{He}(\pi^+, p^3\text{He})$.

function of the p - ${}^3\text{He}$ opening angle, compared with the phase space distribution of $(p\text{ }^3\text{He})$ events calculated with the FOWL Program. The comparison shows that only the 3% of the measured events belongs to the absorption reaction without charge exchange.

Moreover, a coplanarity test which took into account the experimental uncertainties on the incident pion energy and on the measured angles gave a 10% of p and ${}^3\text{He}$ tracks coplanar.

It is then reasonable to assume this value as an upper limit for the cross section of the absorption reaction compared with the charge exchange reaction, in agreement with the results of ref. (19).

As a consequence, because of the values of the $(\pi^0 p\text{ }^3\text{He})$ charge exchange reaction reported in Table I, the cross section values of the $(p\text{ }^3\text{He})$ absorption channel result only a few mb, in the considered energy interval.

It is possible to conclude that the absorption by a quasi deuteron is the principal mechanism in the non radiative capture of π^+ on ${}^4\text{He}$,

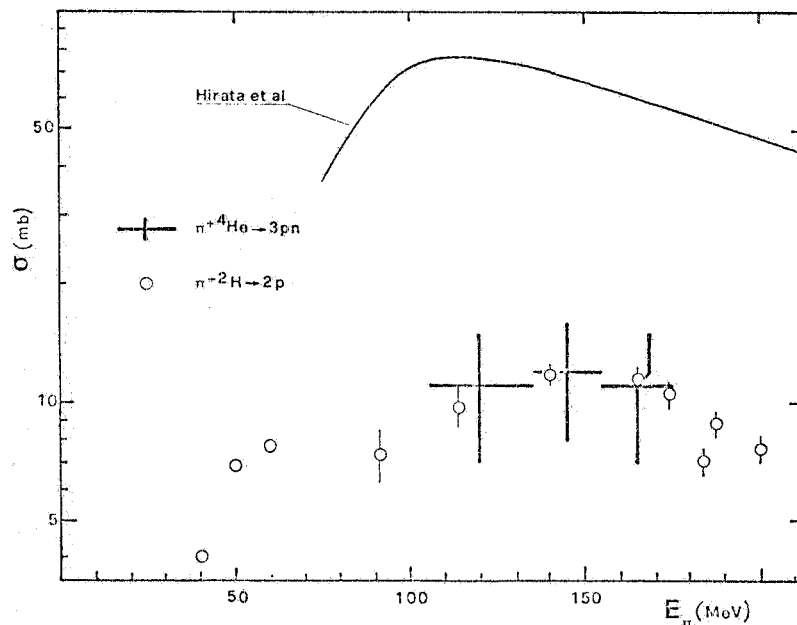


FIG. 6 - ${}^4\text{He}(\pi^+, 3p n)$ cross section versus pion energy. Crosses: present data. Open circles: ${}^2\text{H}(\pi^+, 2p)$ cross section values from ref. (20). The full line represents the absorption cross section calculated in ref. (21).

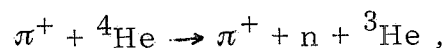
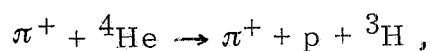
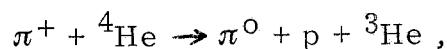
since the cross section values are about ten mb, as reported in Table I. These values are close to the values of the ${}^2\text{H}(\pi^+, 2p)$ reaction⁽²⁰⁾, as shown in Fig. 6.

In the case of quasi deuteron absorption of photons on ${}^4\text{He}$, the ${}^4\text{He}(\gamma, np){}^2\text{H}$ cross section values are also close to the deuteron photodisintegration values⁽¹⁷⁾.

Theoretical calculations of absorption cross section, taking into account the quasi deuteron mechanism, have not yet been performed. The only calculation by Hirata et al.⁽²¹⁾, considering the excitation of Δ -nucleon states, gives values very higher than the experimental ones, as shown in Fig. 6.

4. 3. - Isobaric resonance excitation.

The cross section values of the reactions



at 120, 145 and 165 MeV are reported in Table I.

The three reactions appear as single nucleon removal pion-induced on ${}^4\text{He}$.

The study of the $(\pi, \pi N)$ reactions in the region of the Δ_{33} resonance has a long history. Previous experiments on light nuclei have been performed by counting the yields of radioactive final nuclei⁽²²⁺²⁴⁾ or by detecting γ ray spectra from complex final nuclei⁽²⁵⁾. Experimentally best known are the excitation functions for the reactions ${}^{12}\text{C}(\pi^+, \pi N){}^{11}\text{C}$.

However, both of the above approaches have summed the yields to an unknown number of final states, making it impossible to distinguish the various particle stable states of the residual nucleus.

Only in a recent work⁽²⁶⁾, target nuclei have been chosen to per

mit the study of neutron or proton removal to individual excited final states of several isospin values, by detecting γ radiation from bombarded targets with π^+ .

The same definite situation occurs in the present knock out reactions on ${}^4\text{He}$, which lead to the ground state of ${}^3\text{He}$ (or ${}^3\text{H}$), allowing an unambiguous study of the single-nucleon removal reactions.

A successful direct reaction theory of pion-induced pickup must account for several aspects of the data. The yields to well known final states must be in proportion to the known spectroscopic factors. The dependence on the pion energy must reflect that seen for the basic pion-nucleon interaction and, finally, the ratio of yields from negative and positive pions must reflect the yields known from scattering on a free proton target.

In the present section, the excitation functions and the angular distributions of the three considered knock-out reactions are compared to the results from pion-free nucleon interaction. The yields clearly show the pion-nucleon 3-3 resonance near $(T_\pi)_{\text{lab}} = 180$ MeV. The angular distributions are similar to those obtained on free nucleon. The excitation of the isobaric resonance is stressed by the effective mass distributions of the $(\pi^0 p)$, $(\pi^+ p)$ and $(\pi^+ n)$ systems, which are in agreement with phase space calculations based on the $\Delta(1232)$ resonance production.

Fig. 7 shows the obtained energy behaviour of the charge exchange total cross section ${}^4\text{He}(\pi^+, \pi^0 p){}^3\text{He}$ compared with the experimental results of the charge exchange on free proton $\pi^- + p \rightarrow \pi^0 + n$ obtained by Bugg et al.⁽²⁷⁾. In the figure is also reported the 273 MeV result of Kozodaev et al.⁽⁵⁾. It is clearly shown a maximum around the position of the Δ_{33} resonance.

In Fig. 8 the differential cross section of the charge exchange reaction versus the π^0 scattering angle, at $E_\pi = 165$ MeV, is reported. The data are compared with the cross section values on free pro-

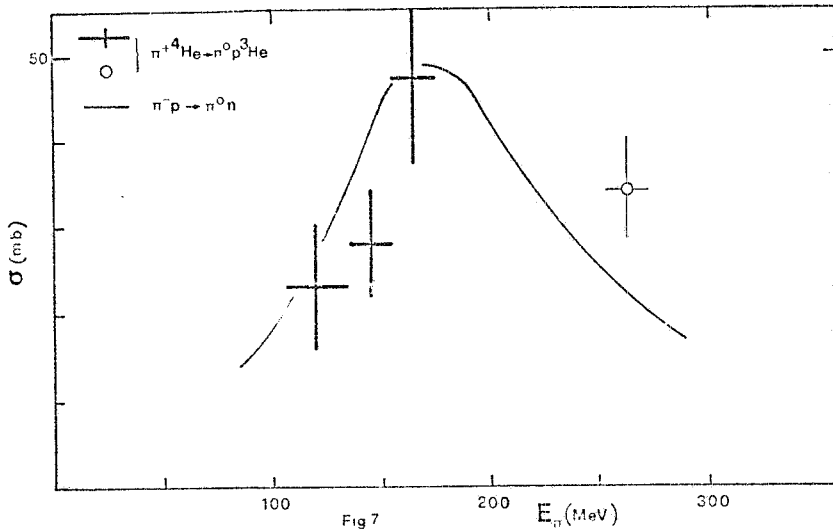


FIG. 7 - ${}^4\text{He}(\pi^+, \pi^0 p){}^3\text{He}$ cross section versus pion energy. Crosses: present data. Open circle: from ref. (5). The full line represents the $\text{H}(\pi^-, \pi^0 n)$ cross section obtained in ref. (27).

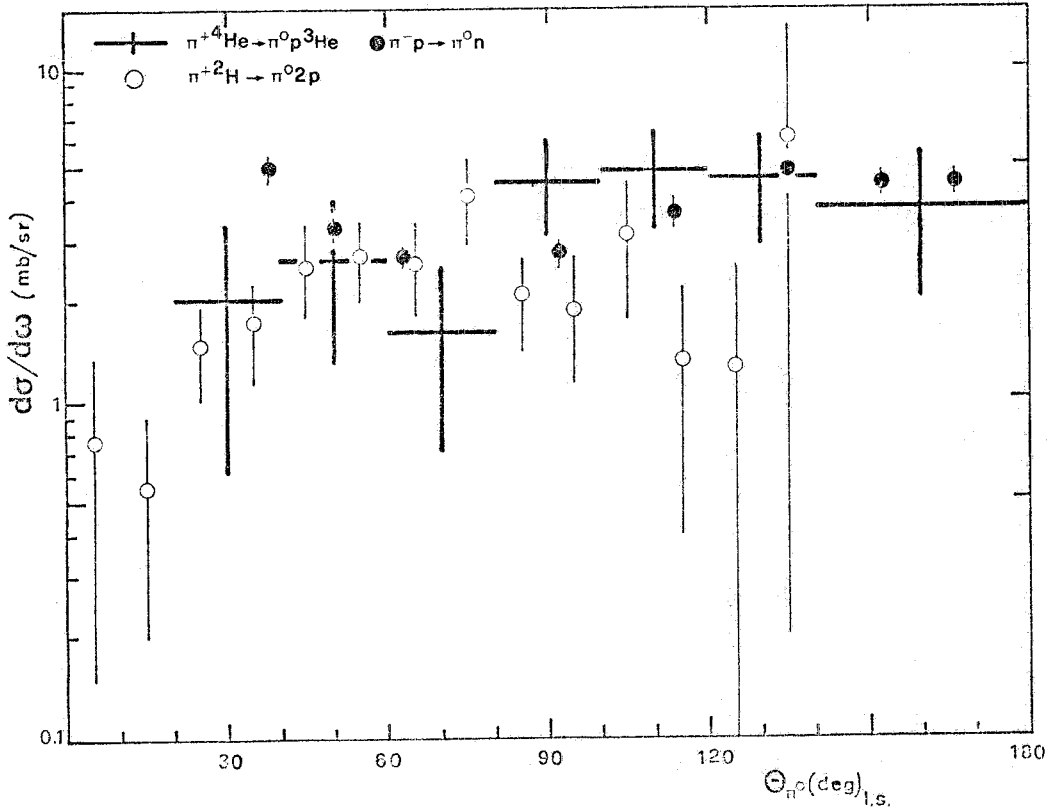


FIG. 8 - ${}^4\text{He}(\pi^+, \pi^0 p){}^3\text{He}$ differential cross section versus π^0 scattering angle at $E_\pi = 165$ MeV (crosses), compared with the $\text{H}(\pi^-, \pi^0 n)$ angular distribution at $E_\pi = 155$ MeV (full circles)(28) and with the ${}^2\text{H}(\pi^+, \pi^0 2p)$ angular distribution at $E_\pi = 183$ MeV (open circles)(29).

ton at $E_\pi = 155$ MeV obtained by Jenefsky et al.⁽²⁸⁾ and with the results of Norem et al.⁽²⁹⁾ for the reaction $\pi^+ + {}^2\text{H} \rightarrow \pi^0 + 2\text{p}$ at 183 MeV. The angular behaviours appear in qualitative agreement.

The role of the isobaric resonance excitation mechanism is stressed in Fig. 9, in which the number of $(\pi^0 \text{p } {}^3\text{He})$ events is plotted against the mass of the $(\pi^0 \text{p})$ system. In the figure the experimental

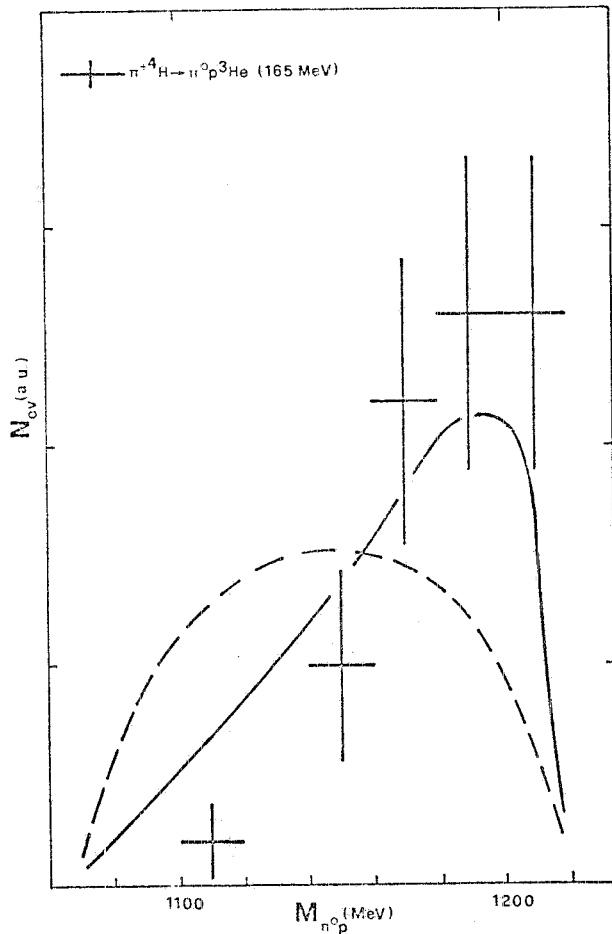


FIG. 9 - Distribution of $(\pi^0 \text{p } {}^3\text{He})$ events as a function of the $(\pi^0 \text{p})$ system effective mass at $E_\pi = 165$ MeV (crosses), compared with the phase space calculations with (full line) and without (dashed line) the hypothesis of $\Delta(1232)$ production.

effective mass distribution is compared with the phase space behaviour calculated with the aid of the FOWL Program⁽⁷⁾ in the hypothesis of $\Delta(1232)$ production. Both experimental and calculated distributions show a significant maximum value at an energy around 1200 MeV, while, if no resonance mechanism is active, the calculated distribution has a symmetric behaviour.

Fig. 10 shows the energy dependence of the obtained total cross section for the ${}^4\text{He}(\pi^+, \pi^+ p){}^3\text{H}$ reaction. In the figure is also reported the 273 MeV result of Kozodaev et al.⁽⁵⁾ and the ${}^4\text{He}(\pi^-, \pi^- n){}^3\text{He}$ cross sections at 153 and 330 MeV obtained by Budagov et al.⁽⁴⁾ and by Kozodaev et al.⁽⁵⁾, respectively. The data are compared with the (π^+, p) process results of Bussey et al.⁽³⁰⁾. A comparison is also made with the knock out process on ${}^{12}\text{C}$: ${}^{12}\text{C}(\pi^-, \pi^- n){}^{11}\text{C}$ using the data of ref. (23). The excitation function shows a resonant behaviour in the region of the (3, 3) resonance on free nucleon; however, the absolute values appear quite lower than the proton data.

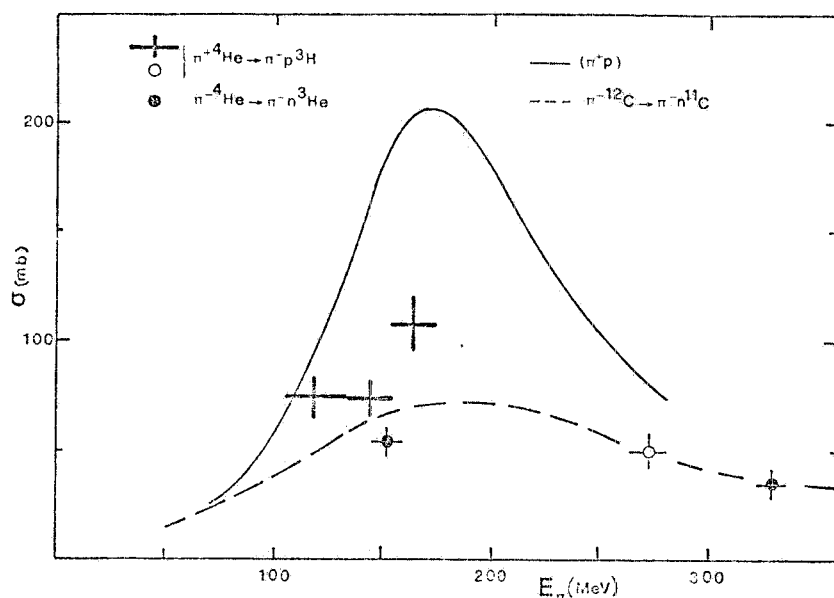


FIG. 10 - ${}^4\text{He}(\pi^+, \pi^+ p){}^3\text{H}$ cross section versus pion energy. Crosses: present data. Open circle: from ref. (5). Full circles: ${}^4\text{He}(\pi^-, \pi^- n){}^3\text{He}$ cross section values from refs. (4, 5). Full line: (π^+, p) data from ref. (30). Dashed line: ${}^{12}\text{C}(\pi^-, \pi^- n){}^{11}\text{C}$ cross section values from ref. (23).

In Fig. 11 the differential cross section of the ${}^4\text{He}(\pi^+, \pi^+ p){}^3\text{H}$ process at $E_\pi = 145$ MeV versus the outgoing pion angle is reported. The angular distribution is compared with the distributions from (π^+, p) scattering⁽³⁰⁾ and from ${}^2\text{H}(\pi^+, p(n))$ reaction⁽²⁹⁾. Again, the three differential cross sections exhibit similar behaviours.

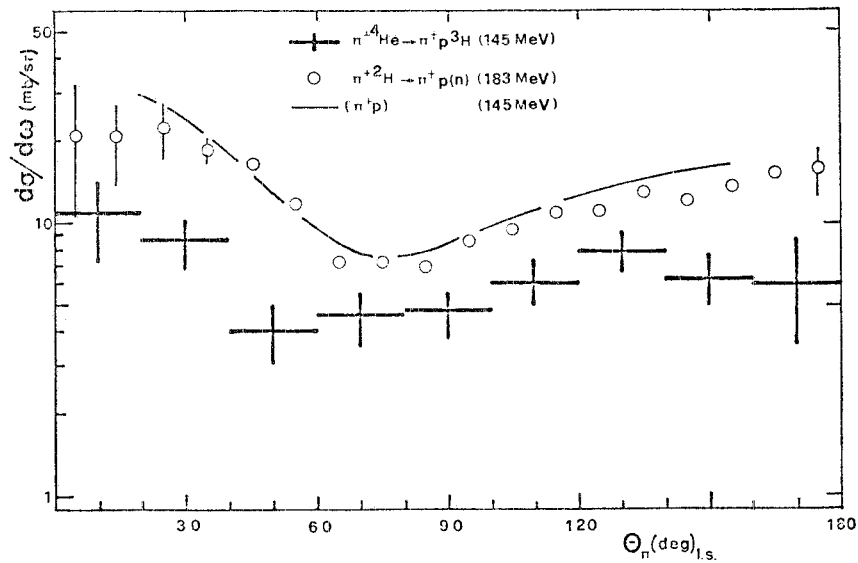


FIG. 11 - ${}^4\text{He}(\pi^+, \pi^+ p){}^3\text{H}$ differential cross section versus the outgoing pion angle at $E_\pi = 145$ MeV (crosses), compared with the (π^+, \bar{p}) angular distribution at $E_\pi = 145$ MeV (full line)⁽³⁰⁾ and with the ${}^2\text{H}(\pi^+, p(n))$ angular distribution at $E_\pi = 183$ MeV (open circles)⁽²⁹⁾.

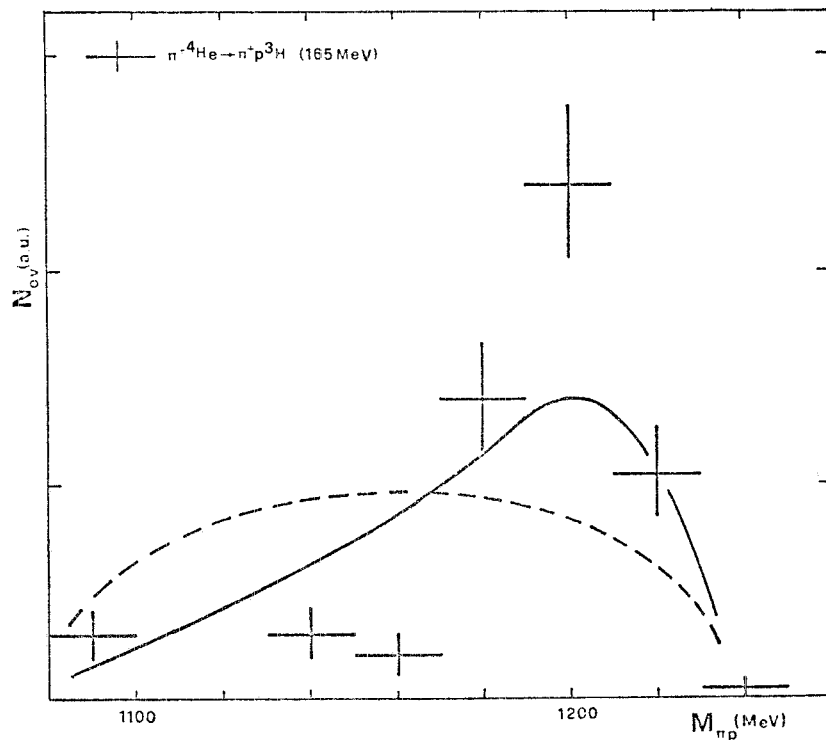


FIG. 12 - Distribution of $(\pi^+ p {}^3\text{H})$ events as a function of the $(\pi^+ p)$ system effective mass at $E_\pi = 165$ MeV (crosses), compared with the phase space calculations with (full line) and without (dashed line) the hypothesis of $\Delta(1232)$ production.

In Fig. 12 the number of $(\pi^+ p \ ^3\text{H})$ events is plotted versus the effective mass of the $(\pi^+ p)$ system. The experimental mass distribution compares favorably with a phase space calculation which takes into account the excitation of the Δ resonance.

Fig. 13 shows the energy dependence of the obtained total cross section of the $^4\text{He}(\pi^+, \pi^+ n)^3\text{He}$ reaction. In the figure is also repor-

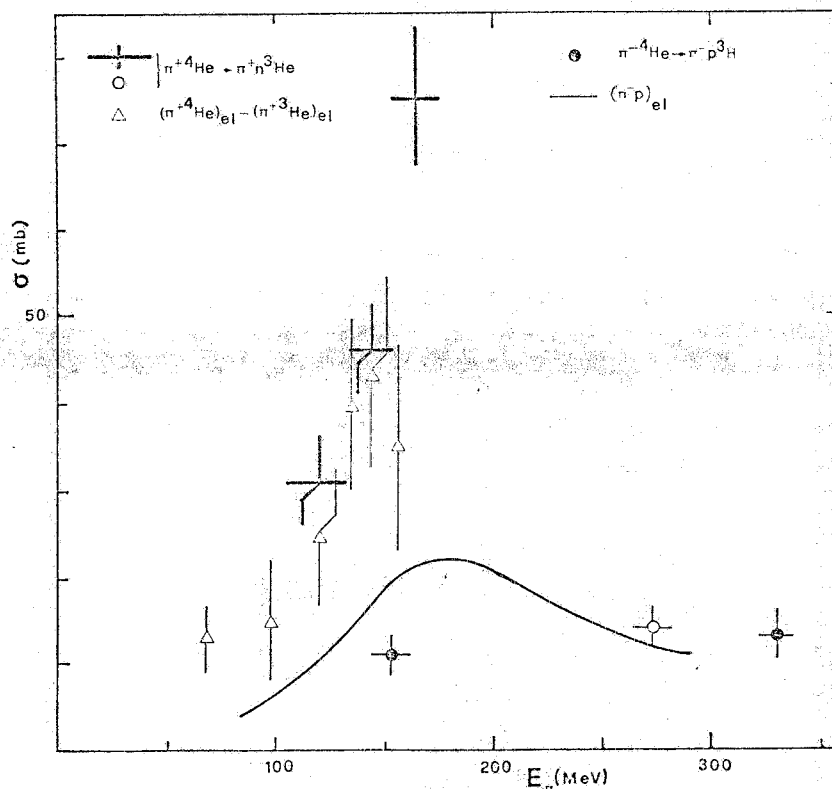


FIG. 13 - $^4\text{He}(\pi^+, \pi^+ n)^3\text{He}$ cross section versus pion energy. Crosses: present data. Open circle: from ref. (5). Full circles: $^4\text{He}(\pi^-, \pi^- n)^3\text{He}$ cross section values from refs. (4, 5). Full line: (π^-, p) data from ref. (30). Triangles: $\sigma(\pi^+, ^4\text{He})_{el} - \sigma(\pi^+, ^3\text{He})_{el}$ from ref. (8).

ted the 273 MeV result of Kozodaev et al.⁽⁵⁾ and the $(\pi^- n \ ^3\text{He})$ data at 153 and 330 MeV obtained, respectively, by Budagov et al.⁽⁴⁾ and by Kozodaev et al.⁽⁵⁾. The data are compared with the (π^-, p) results from Bussey et al.⁽³⁰⁾. A comparison is also made with the cross section values concerning the difference $\sigma(\pi^+, ^4\text{He})_{el} - \sigma(\pi^+, ^3\text{He})_{el}$, as obtained in ref. (8). The resonant mechanism is again confirmed.

Fig. 14 shows the differential cross section of the ${}^4\text{He}(\pi^+, \pi^+ n){}^3\text{He}$ reaction, at $E_\pi = 145$ MeV, versus the outgoing pion angle. The distribution is compared with the (π^-, p) and ${}^2\text{H}(\pi^+, n(p))$

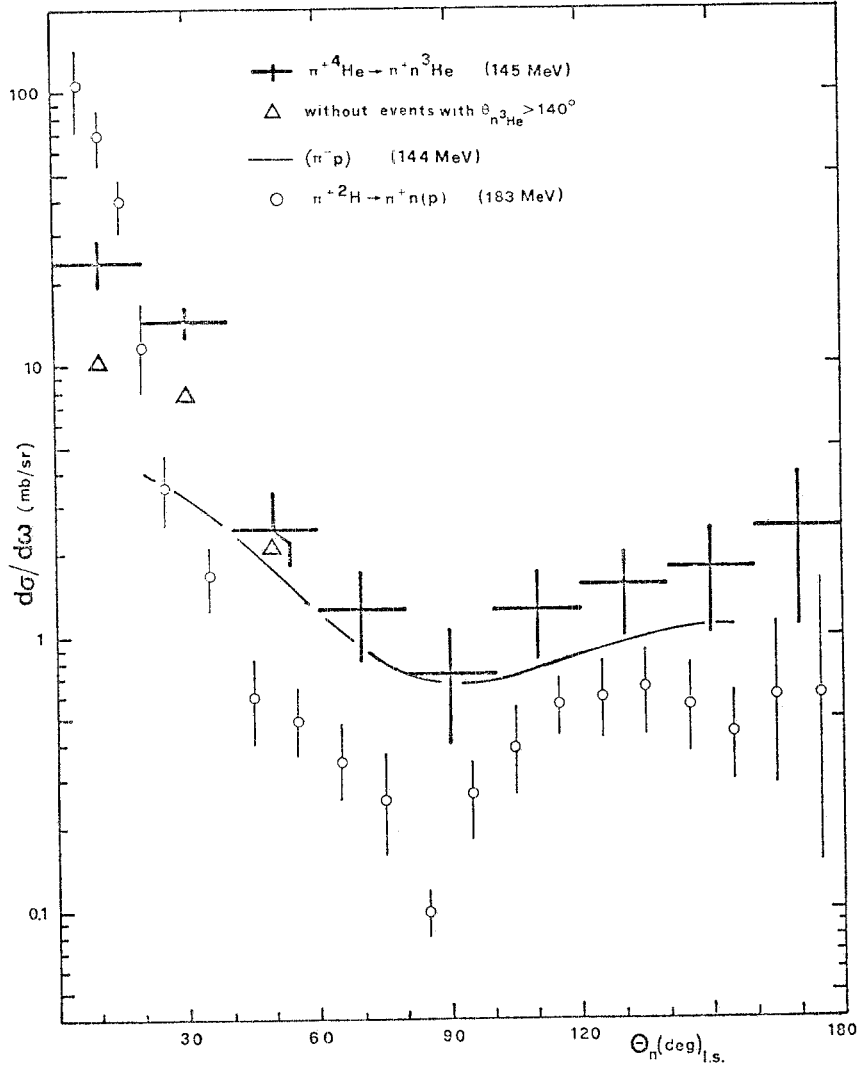


FIG. 14 - ${}^4\text{He}(\pi^+, \pi^+ n){}^3\text{He}$ differential cross section versus the outgoing pion angle at $E_\pi = 145$ MeV (crosses), compared with the (π^-, p) angular distribution at $E_\pi = 144$ MeV (full line)(30) and with the ${}^2\text{H}(\pi^+, n(p))$ angular distribution at $E_\pi = 183$ MeV (open circles)(29). The triangles represent the differential cross section values calculated without the events with the n - ${}^3\text{He}$ opening angle larger than 140° .

distributions obtained by Bussey et al.(30) and by Norem et al.(29). There is a qualitative agreement between the angular behaviours. However, for $\theta_\pi \lesssim 50^\circ$, the $(\pi^+ n {}^3\text{He})$ values are sensibly higher than

those of the free nucleon distribution.

Finally, in Fig. 15 the number of $(\pi^+ n \ ^3\text{He})$ events is plotted versus the effective mass of the $(\pi^+ n)$ system. As in the cases of the

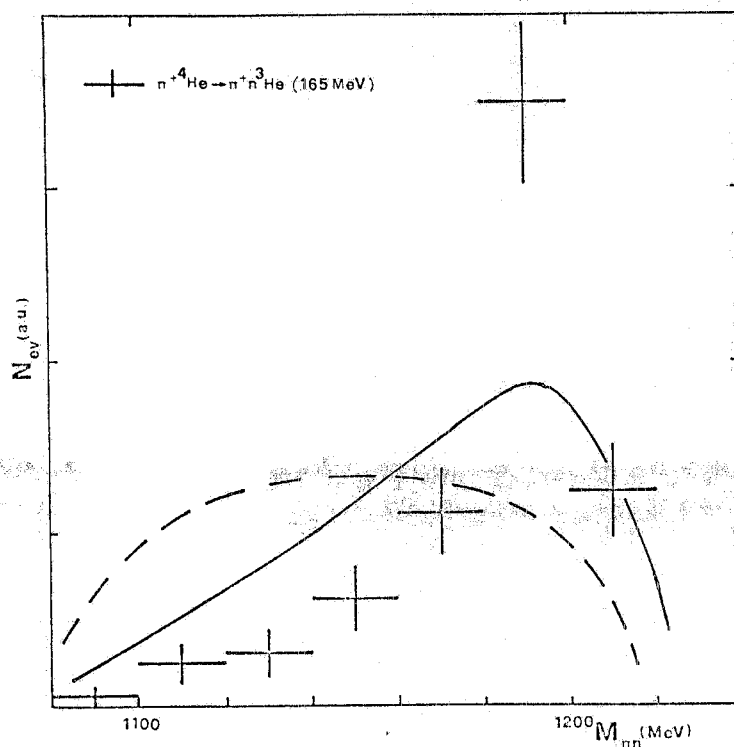


FIG. 15 - Distribution of $(\pi^+ n \ ^3\text{He})$ events as a function of the $(\pi^+ n)$ system effective mass at $E_\pi = 165$ MeV (crosses), compared with the phase space calculations with (full line) and without (dashed line) the hypothesis of $\Delta(1232)$ production.

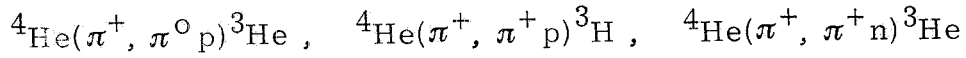
mass distributions of the $(\pi^0 p)$ and $(\pi^+ p)$ systems, the experimental values do agree with a phase space distribution calculated taking into account the excitation of the Δ resonance, while the calculation without the isobaric resonance excitation appear far from the experimental result.

On the contrary, as we have seen in Fig. 3 (upper part) and in Fig. 6, the energy behaviours of the $^4\text{He}(\pi^+, \pi^+ 2p 2n)$ and $^4\text{He}(\pi^+, 3pn)$ cross sections do not exhibit any marked bump in the Δ_{33} region. The same flat behaviour is exhibited by the double charge exchange $^4\text{He}(\pi^+, \pi^- 4p)$ cross section, as obtained in ref. (31).

It is possible to conclude that the resonance behaviour of the total inelastic (π^+ , ^4He) cross section (see Fig. 2) can be essentially ascribed to the isobaric resonance excitation mechanism of the (π^+ , $\pi^0\text{p}$), (π^+ , $\pi^+\text{p}$) and (π^+ , $\pi^+\text{n}$) reaction channels.

4.4. - Three nucleon exchange mechanism.

For the three knock out reactions on ^4He considered in the previous section :



we define the ratio

$$R_{\text{He}} = \frac{\sigma_{\pi^+\text{p}}^3\text{H}}{\sigma_{\pi^+\text{n}}^3\text{He} + \sigma_{\pi^0\text{p}}^3\text{He}} .$$

In Table II the R_{He} ratios at the energies of the experiment are reported, together with the 273 MeV value from Kozodaev et al. data⁽⁵⁾.

TABLE II

E_{π} (MeV)	R_{He}
120 ± 15	1.37 ± 0.36
145 ± 10	0.99 ± 0.26
165 ± 10	0.88 ± 0.20
273 ± 7	1.04 ± 0.30

As it can be seen from the Table, the simple plane wave impulse approximation (PWIA), even in the case of a nucleus as light as ^4He , fails to reproduce the experimental values of R_{He} (in fact a value of about 3 is expected on the 3-3 resonance). This apparent conflict indicates the considerable role of the initial and/or final-state interaction in pion induced knock out reactions.

It is known that all the measured ratios of yields by π^- and π^+

of $(\pi, \pi N)$ reactions on light nuclei present this significant puzzle⁽²²⁺²⁶⁾.

If nuclear absorption effects are simply included by allowing the exiting nucleon to charge exchange, the simple ratio of 3 on the resonance is considerably modified^(32, 33) and the predictions compare reasonably well with the observed ratios for ${}^6\text{Li}$, ${}^8\text{Li}$, ${}^{12}\text{C}$ ($T=0$) and ${}^{12}\text{C}$ ($T=1$). Only the valence $p_{3/2}$ nucleons are indicated in this calculation.

In the case of such a system as ${}^4\text{He}$, a simple theoretical model which incorporates the three-nucleon exchange mechanism in the plane wave impulse approximation, in addition to the one-nucleon mechanism, has been introduced by Mach et al.⁽³⁴⁾. By the aid of this model, it is possible to explain qualitatively both the R_{He} ratios and the differential cross section behaviours.

In Fig. 16 the experimental ratios are compared with the PWIA calculation and with the model which takes into account also the three nucleon exchange mechanism. The results from this last calculation lie rather close to the experimental ones, much closer than the PWIA values.

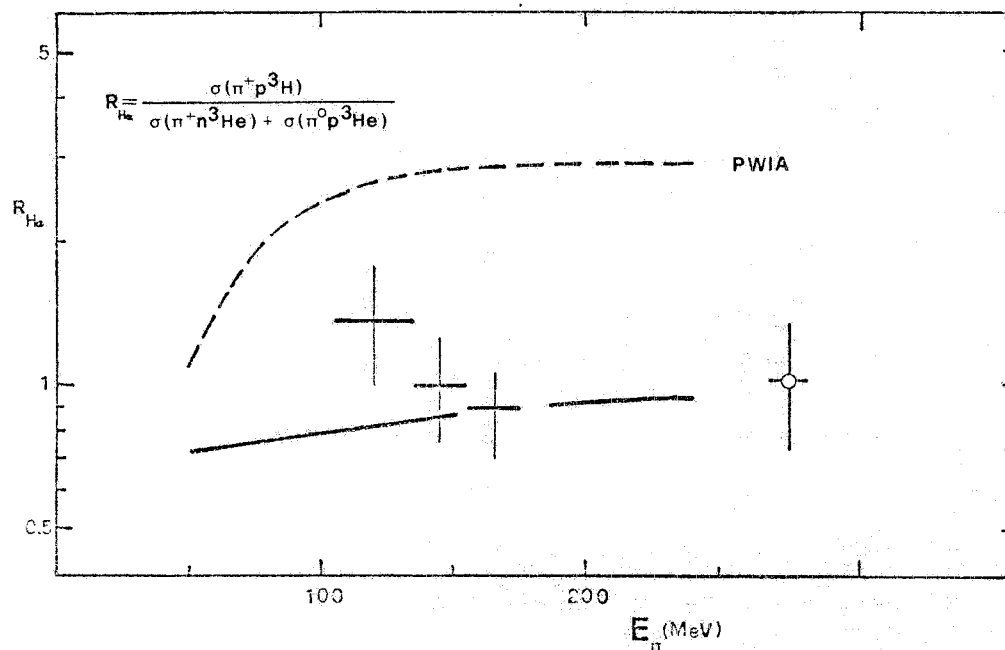


FIG. 16 - Energy dependence of the experimental R_{He} ratio (crosses) compared with the three-nucleon exchange model (full line) and with the PWIA prediction (dashed line) from ref. (34). Open circle: from ref. (5).

In Fig. 17 is reported the π^0 angular distribution in the charge exchange reaction ${}^4\text{He}(\pi^+, \pi^0 p){}^3\text{He}$ at $E_\pi = 165$ MeV, compared with the result of the three nucleon exchange calculation. The present mo

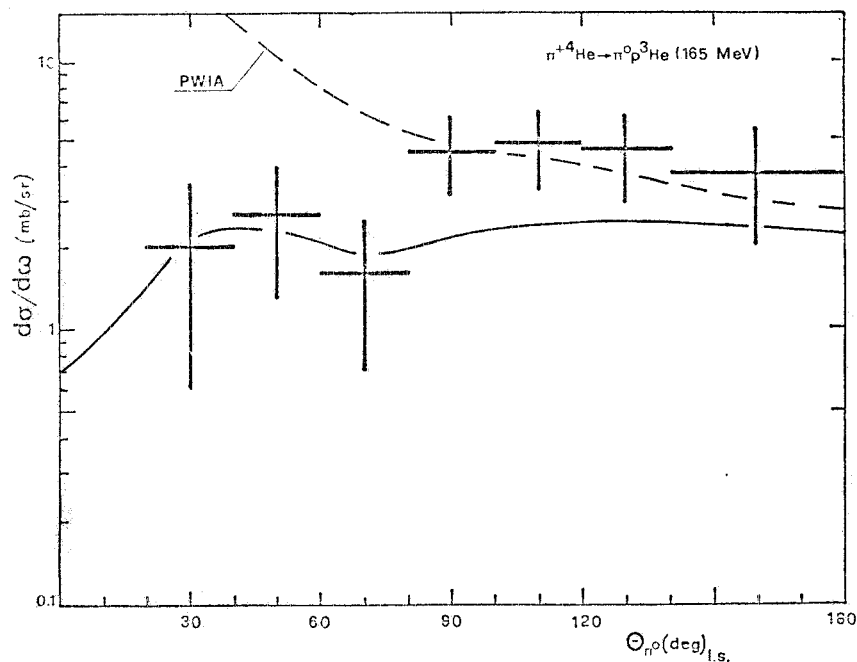


FIG. 17 - ${}^4\text{He}(\pi^+, \pi^0 p){}^3\text{He}$ differential cross section as a function of π^0 scattering angle, at $E_\pi = 165$ MeV (crosses), compared with the three-nucleon exchange model (full line) and with the PWIA prediction (dashed line) from ref. (34).

del describes the shape of the differential cross section much better than the PWIA does (dashed line in the figure). The model predicts correctly the position of the first maximum as well as the build up in the backward angular region.

The comparison between the angular distributions of the $(\pi^+ p {}^3\text{H})$ and $(\pi^+ n {}^3\text{He})$ knock out events with the results of the three nucleon exchange calculation has been reported in ref. (34). For these two reactions only a qualitative agreement has been found.

4.5. - Clustering effects.

Clustering effects in $(\pi^+, {}^4\text{He})$ inelastic interactions can be investigated searching for correlated emissions of systems such as nucleon-

-recoil nucleus in single-nucleon removal reactions as ${}^4\text{He}(\pi^+, \pi^0\text{p}){}^3\text{He}$, ${}^4\text{He}(\pi^+, \pi^+\text{p}){}^3\text{H}$ and ${}^4\text{He}(\pi^+, \pi^+\text{n}){}^3\text{He}$.

Fig. 18 shows the distribution of the events of the three above reactions as a function of the opening angle between the nucleon and the recoil nucleus at $E_\pi = 145$ MeV, normalized to the respective cross sections.

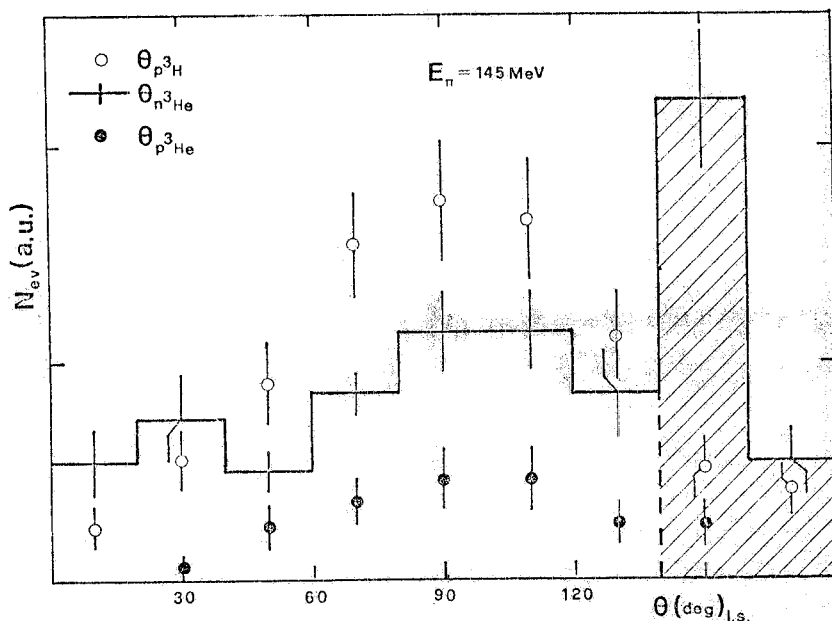


FIG. 18 - Distributions of $(\pi^+\text{p}{}^3\text{H})$ events (open circles); $(\pi^+\text{n}{}^3\text{He})$ events (crosses); $(\pi^0\text{p}{}^3\text{He})$ events (full circles) as functions of the opening angle between the nucleon and the recoil nucleus, normalized to the respective cross sections. The dashed histogram represents the distribution of $(\pi^+\text{n}{}^3\text{He})$ events with $\theta_{\text{n}{}^3\text{He}} > 140^\circ$.

The distributions of $(\pi^0\text{p}{}^3\text{He})$ events and of $(\pi^+\text{p}{}^3\text{H})$ events have symmetrical behaviours with a large maximum around 90° .

On the contrary, the distribution of $(\pi^+\text{n}{}^3\text{He})$ events is clearly peaked around $\theta_{\text{n}{}^3\text{He}} \simeq 150^\circ$, which indicates a strong correlation between the neutron and the ${}^3\text{He}$ recoil nucleus. Similar correlated neutron-deuteron and neutron-tritium pair emission have been observed in π^- capture on ${}^{12}\text{C}$ (35).

The $(\pi^+ n \ ^3\text{He})$ correlated events, i. e. with $\theta_{n \ ^3\text{He}} \gtrsim 140^\circ$, are the 32% of the total number of events (dashed area in Fig. 18). The contribution of this events is significant at an angle of the outgoing pion $\theta_{\pi^+} \lesssim 50^\circ$. This fact is shown in Fig. 14 in which the π^+ angular distribution of the $^4\text{He}(\pi^+, \pi^+ n)^3\text{He}$ reaction is reported. As it is possible to see, the exclusion of the events with $\theta_{n \ ^3\text{He}} \gtrsim 140^\circ$ becomes significant only for $\theta_{\pi^+} \lesssim 50^\circ$.

Further informations on the found correlation can be deduced from the analysis of the energy distributions of the particles emitted in the "clustering" reaction by selecting the events with $\theta_{n \ ^3\text{He}} < 140^\circ$ from those with $\theta_{n \ ^3\text{He}} > 140^\circ$. In the first class of events ($\theta < 140^\circ$), π^+ , n and ^3He have, respectively, the average energies :

$$\bar{E}_{\pi^+} = 102.8 \text{ MeV}; \quad \bar{E}_n = 16.6 \text{ MeV}; \quad \bar{E}_{^3\text{He}} = 6.9 \text{ MeV},$$

as it can be deduced from Fig. 19.

In the second class of events ($\theta > 140^\circ$), the average energies are, respectively :

$$\bar{E}_{\pi^+} = 89.6 \text{ MeV}; \quad \bar{E}_n = 27.4 \text{ MeV}; \quad \bar{E}_{^3\text{He}} = 7.3 \text{ MeV},$$

as it can be deduced from the dashed areas of Fig. 19. This means that the operating of the correlation (for $\theta_{n \ ^3\text{He}} \gtrsim 140^\circ$) is characterized by a stronger relative energy of the n- ^3He pair (and a lower scattered-pion energy), compared to the energy of the uncorrelated events ($\theta_{n \ ^3\text{He}} \lesssim 140^\circ$).

Fig. 20 gives the energy distributions of π^0 , p and ^3He in the "non clustered" reaction $^4\text{He}(\pi^+, \pi^0 p)^3\text{He}$.

Fig. 21 gives the energy distributions of π^+ , p and ^3H in the other "non clustered" reaction $^4\text{He}(\pi^+, \pi^+ p)^3\text{H}$.

Moreover, if we analyze the average effective mass of the (n ^3He) system, selecting again between the events with $\theta_{n \ ^3\text{He}} \gtrsim 140^\circ$, we find

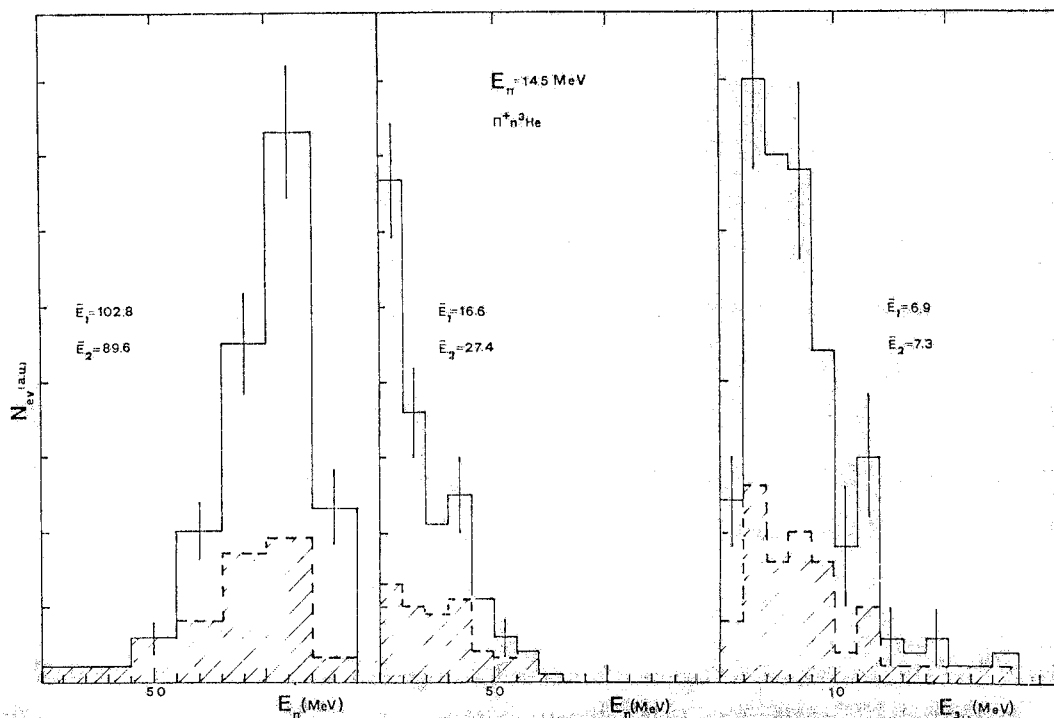


FIG. 19 - Energy distributions of the particles emitted in the ${}^4\text{He}(\pi^+, \pi^+n){}^3\text{He}$ reaction at $E_\pi = 145$ MeV. Full areas: $(\pi^+n){}^3\text{He}$ events with $\theta_{n{}^3\text{He}} < 140^\circ$. Dashed areas: $(\pi^+n){}^3\text{He}$ events with $\theta_{n{}^3\text{He}} > 140^\circ$. \bar{E}_1 : mean energy of the emitted particle in a $(\pi^+n){}^3\text{He}$ event with $\theta_{n{}^3\text{He}} < 140^\circ$. \bar{E}_2 : mean energy of the emitted particle in a $(\pi^+n){}^3\text{He}$ event with $\theta_{n{}^3\text{He}} > 140^\circ$.

$$\bar{M}_{\theta < 140^\circ} = 3760 \text{ MeV} , \quad \bar{M}_{\theta > 140^\circ} = 3780 \text{ MeV} ,$$

as it can be deduced from Fig. 22.

The mass difference of 20 MeV is just close to the neutron binding energy in the ${}^4\text{He}$ nucleus.

In Fig. 23 the effective mass distributions of the uncorrelated $(p{}^3\text{He})$ and $(p{}^3\text{H})$ systems are reported.

In conclusion, as far the $(\pi^+n){}^3\text{He}$ events are concerned, in one third of the cases there are $(n{}^3\text{He})$ clustering effects, with the neutron and the ${}^3\text{He}$ emitted back to back. The effective mass difference has a value near the binding energy of the neutron in the considered nucleus.

On the contrary, no angular correlations are evident for the $(p{}^3\text{He})$ and $(p{}^3\text{H})$ pairs.

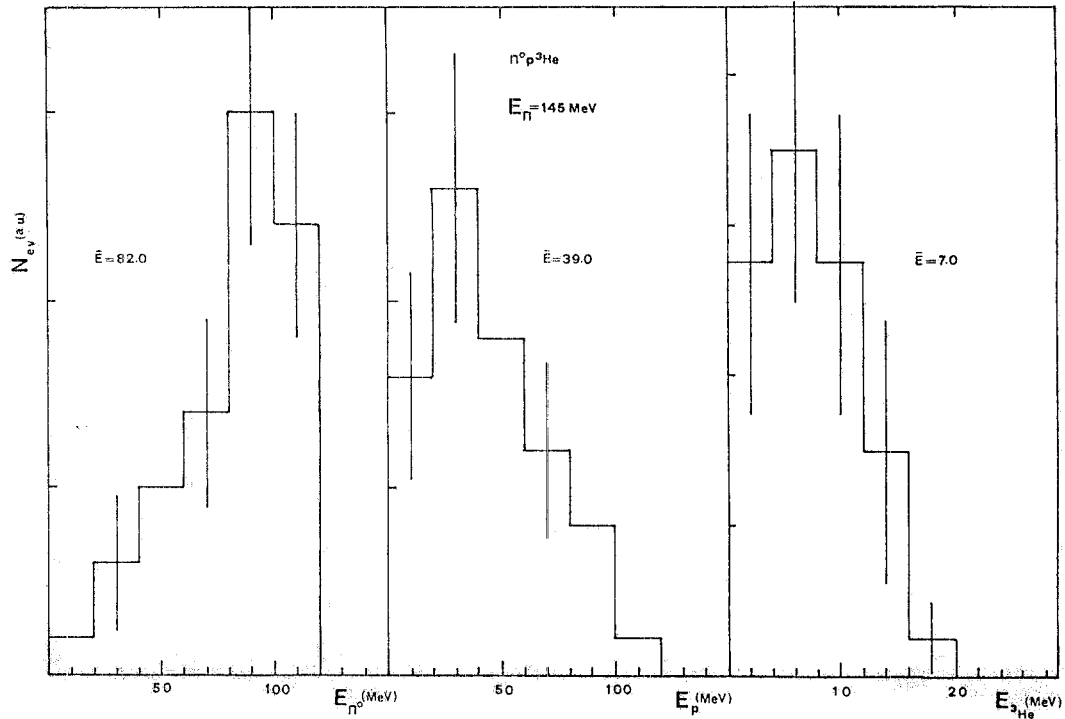


FIG. 20 - Energy distributions of the particles emitted in the $^4\text{He}(\pi^+, \pi^0 p)^3\text{He}$ reaction. \bar{E} : mean energy of the emitted particle. $E_\pi = 145 \text{ MeV}$.

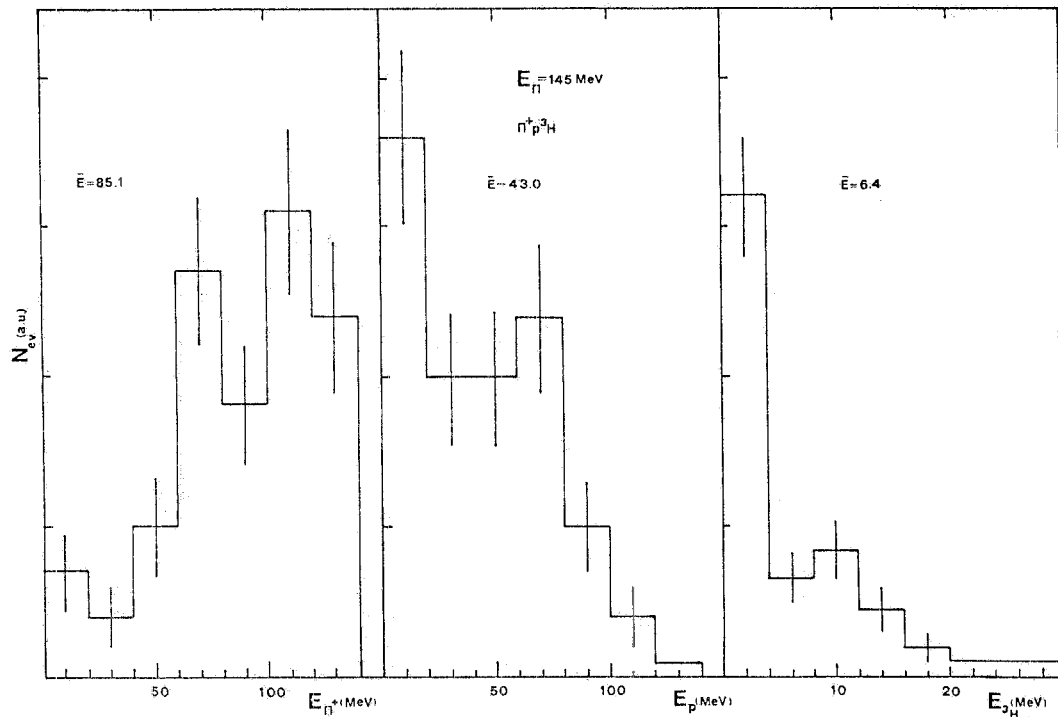


FIG. 21 - Energy distributions of the particles emitted in the $^4\text{He}(\pi^+, \pi^+ p)^3\text{H}$ reaction. \bar{E} : mean energy of the emitted particle. $E_\pi = 145 \text{ MeV}$.

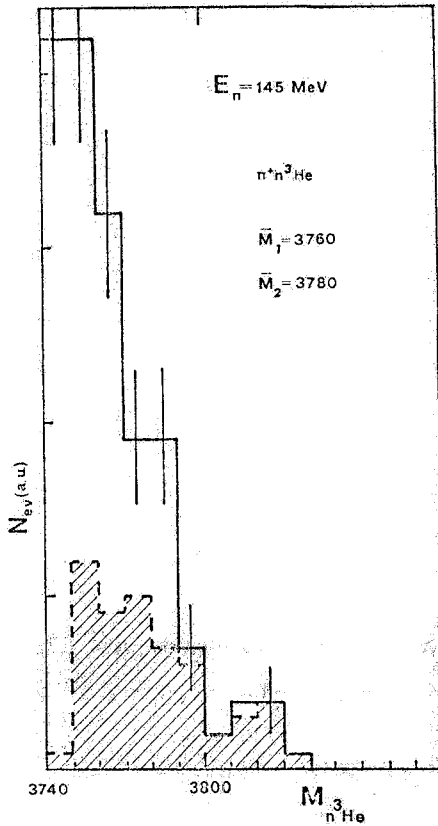


FIG. 22 - Distributions of $(\pi^+ n^3\text{He})$ events as functions of the effective mass of the $(n^3\text{He})$ system, at $E_\pi = 145$ MeV. Full area: events with $\theta_{n^3\text{He}} < 140^\circ$.

Dashed area: events with $\theta_{n^3\text{He}} > 140^\circ$. \bar{M}_1 : average effective mass of $(\theta_{n^3\text{He}} < 140^\circ)$ events. \bar{M}_2 : average effective mass of $(\theta_{n^3\text{He}} > 140^\circ)$ events.

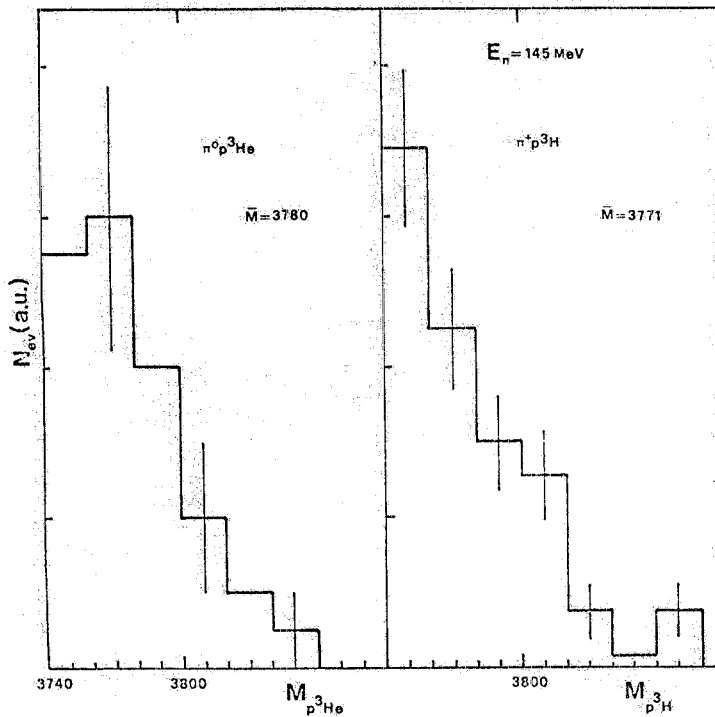


FIG. 23 - Distributions of $(\pi^0 p^3\text{He})$ and $(\pi^+ p^3\text{H})$ events as functions of the effective mass of the $(p^3\text{He})$ and $(p^3\text{H})$ systems, respectively. \bar{M} : average effective mass of the system. $E_\pi = 145$ MeV.

Similarly, in ${}^4\text{He}(\gamma, np){}^2\text{H}$ reaction, angular correlation has been found⁽²⁰⁾ for the $(n{}^2\text{H})$ pair, but not for the $(p{}^2\text{H})$ pair.

It is possible to conclude, in agreement with the results obtained by Lee et al.⁽³⁵⁾ in the π^- capture on ${}^{12}\text{C}$, that (n, p) , $(n{}^2\text{H})$, $(n{}^3\text{H})$ and $(n{}^3\text{He})$ pairs can be emitted correlated from light nuclei.

For $(p{}^2\text{H})$, $(p{}^3\text{H})$ and $(p{}^3\text{He})$ pairs the angular correlation is negligible, because of Coulomb effects and different interactions in final states.

REFERENCES.

- (1) - L. Busso, S. Costa, R. Garfagnini, G. Piragino, R. Barbini, C. Guaraldo and R. Scrimaglio, Nuclear Instr. and Meth. 102, 1 (1972).
- (2) - F. Balestra, L. Busso, R. Garfagnini, G. Piragino, R. Barbini, C. Guaraldo, R. Scrimaglio, I. V. Falomkin, M. M. Kulyukin and Yu. A. Shcherbakov, Nuclear Instr. and Meth. 119, 347 (1974).
- (3) - R. Barbini, L. Busso, S. Costa, R. Garfagnini, C. Guaraldo, G. Piragino and R. Scrimaglio, Frascati Report LNF-72/62 (1972), and in 'Few Particle Problems in the Nuclear Interaction', Los Angeles (North Holland, 1972), pag. 866; F. Balestra, L. Busso, R. Garfagnini, G. Piragino, R. Barbini, C. Guaraldo and R. Scrimaglio, Lett. Nuovo Cimento 15, 535, 542 (1976).
- (4) - Yu. A. Budagov, P. F. Ermolov, E. A. Kushnirenko and V. I. Moskalev, Sov. Phys. - JETP 15, 824 (1962).
- (5) - M. S. Kozodaev, M. M. Kulyukin, R. M. Sulyaev, A. I. Filippov and Yu. A. Shcherbakov, Sov. Phys. - JETP 11, 300 (1960).
- (6) - H. E. Jackson, S. B. Kaufman, L. Meyer-Schützmeister, J. P. Schiffer, S. L. Tabor, S. E. Vigdor, J. N. Worthington, L. L. Rutledge jr., R. E. Segel, R. L. Burman, P. A. M. Gram, R. P. Redwine and M. A. Yates, Phys. Rev. 16C, 730 (1977); Yu. R. Gismatullin, I. A. Lantsev and V. I. Ostroumov, Sov. J. Nucl. 26, 126 (1977).
- (7) - F. James, Report CERN 68-15 (1968); Program Library, W505 (1970).

- (8) - Yu. A. Shcherbakov, T. Angelescu, I. V. Falomkin, M. M. Kulyukin, V. I. Lyashenko, R. Mach, A. Mihul, N. M. Kao, F. Nichitiu, G. B. Pontecorvo, V. K. Sarycheva, M. G. Sapozhnikov, M. Semerdjieva, T. M. Troshev, N. I. Trosheva, F. Balestra, L. Busso, R. Garfagnini and G. Piragino, *Nuovo Cimento* 31A, 249 (1976); I. V. Falomkin, V. I. Lyashenko, G. B. Pontecorvo, M. G. Sapozhnikov, Yu. A. Shcherbakov, F. Balestra, R. Garfagnini, G. Piragino, T. Angelescu, A. Mihul and F. Nichitiu, *Nuovo Cimento* 43A, 219 (1978).
- (9) - E. C. Fowler, W. B. Fowler, R. P. Shutt, A. M. Thorndike and W. L. Whittemore, *Phys. Rev.* 91, 135 (1953).
- (10) - K. M. Crowe, A. Fainberg, J. Miller and A. S. L. Parsons, *Phys. Rev.* 180, 1349 (1969).
- (11) - M. E. Nordberg and K. F. Kinsey, *Phys. Letters* 20, 692 (1966).
- (12) - F. Binon, P. Duteil, M. Gouarnere, L. Hugon, J. Jansen, J. -P. Lagnaux, H. Palevsky, J. -P. Peigneux, M. Spighel and J. -P. Stroot, *Nuclear Phys.* 298A, 499 (1978).
- (13) - R. H. Landau, *Phys. Rev.* 15C, 2127 (1977).
- (14) - M. Wakamatsu, *Nuclear Phys.* 312A, 427 (1978).
- (15) - J. P. Maillet, J. P. Dedonder and C. Schmit, *Nuclear Phys.* 316A, 267 (1979).
- (16) - C. Wilkin, C. R. Cox, J. J. Domingo, K. Gabathuler, E. Pedroni, J. Rohlin, P. Schwaller and N. W. Tanner, *Nuclear Phys.* 62B, 61 (1973).
- (17) - F. Balestra, E. Bollini, L. Busso, R. Garfagnini, C. Guaraldo, G. Piragino, R. Scrimaglio and A. Zanini, *Nuovo Cimento* 38A, 145 (1977), and Frascati Report LNF-78/28 (1978).
- (18) - S. C. Chakravartty and J. Hebert, *Phys. Rev.* 16C, 1097 (1977).
- (19) - F. Calligaris, C. Cernigoi, I. Gabrielli and F. Pellegrini, in 'High Energy Physics and Nuclear Structure' (Plenum Press, 1970), pag. 367.
- (20) - C. Richard-Serre, W. Hirt, D. F. Measday, E. G. Michaelis, M. J. M. Saltmarsch and P. Skarek, *Nuclear Phys.* 20B, 413 (1970), and literature thereby quoted; B. M. Preedom, C. W. Darden, R. D. Edge, T. Marks, M. J. Saltmarsch, K. Gabathuler, E. E. Gross, C. A. Ludemann, P. Y. Bertin, M. Blecher, K. Gotow, J. Alster, R. L. Burman, J. P. Perroud and R. P. Redwine, *Phys. Rev.* 17C, 1402 (1978).
- (21) - M. Hirata, F. Lenz and K. Yazaki, *Ann. Phys.* 108, 116 (1977).
- (22) - D. T. Chivers, E. M. Rimmer, B. W. Allardyce, R. C. Witcomb, J. J. Domingo and N. W. Tanner, *Phys. Letters* 26B, 574 (1968); *Nuclear Phys.* 126A, 129 (1969).
- (23) - B. J. Dropevsky, G. W. Butler, C. J. Orth, R. A. Williams, G. Friedlander, M. A. Yates and S. B. Kauman, *Phys. Rev. Letters* 34, 821 (1975); L. H. Batist, V. D. Vitman, V. P. Koptev, M. M. Makarov, A. A. Naberezhnov, V. V. Nelyubin, G. Z. Obrant, V. V. Sarantsev and G. V. Shcherbakov, *Nuclear Phys.* 254A, 480 (1975).

- (24) - N. P. Jacob and S. S. Markowitz, *Phys. Rev.* 13C, 754 (1976).
- (25) - B. G. Lieb, H. S. Plendl, H. O. Funstein, W. J. Kossler and C. E. Stronach, *Phys. Rev. Letters* 34, 965 (1975); B. J. Lieb and H. O. Funstein, *Phys. Rev.* 10C, 1753 (1974).
- (26) - C. L. Morris, R. L. Boudrie, J. J. Kraushaar, R. J. Peterson, R. A. Ristinen, G. R. Smith, J. E. Bolger, W. J. Braithwaite, C. F. Moore and L. E. Smith, *Phys. Rev.* 17C, 227 (1978).
- (27) - D. V. Bugg, P. J. Bussey, D. R. Dance, A. R. Smith, A. A. Carter and J. R. Williams, *Nuclear Phys.* 26B, 588 (1971).
- (28) - R. F. Jenefsky, C. Joseph, M. T. Tran, B. Vaucher, E. Winkelmann, T. Bressani, E. Chiavassa, G. Venturello, H. Schmitt and C. Zupancic, *Nuclear Phys.* 290A, 407 (1977).
- (29) - J. H. Norem, *Nuclear Phys.* 33B, 512 (1971).
- (30) - P. J. Bussey, J. R. Carter, D. R. Dance, D. V. Bugg, A. A. Carter and A. M. Smith, *Nuclear Phys.* 58B, 363 (1973).
- (31) - I. V. Falomkin, V. I. Lyashenko, G. B. Pontecorvo, Yu. A. Shcherbakov, M. Albu, T. Angelescu, O. Balea, A. Mihul, F. Nichitiu, A. Seraru, F. Balestra, R. Garfagnini, G. Piragino, C. Guaraldo and R. Scrimaglio, *Lett. Nuovo Cimento* 16, 525 (1976).
- (32) - M. M. Sternheim and R. R. Silbar, *Phys. Rev. Letters* 34, 824 (1975).
- (33) - R. R. Silbar, J. N. Ginocchio and M. M. Sternheim, *Phys. Rev.* 15C, 371 (1977); R. R. Silbar, *Phys. Rev.* 15C, 1158 (1977).
- (34) - R. Mach, M. G. Sapozhnikov, C. Guaraldo, R. Scrimaglio, F. Balestra, R. Garfagnini and G. Piragino, *Nuovo Cimento* 45A, 325 (1978).
- (35) - D. M. Lee, R. C. Minehart, S. E. Sobotka and K. O. H. Ziock, *Nuclear Phys.* 197A, 106 (1972).